Quantum randomness certified by the uncertainty principle

Giuseppe Vallone, Davide G. Marangon, Marco Tomasin, and Paolo Villoresi
Department of Information Engineering, University of Padova, I-35131 Padova, Italy
(Received 9 February 2014; revised manuscript received 1 November 2014; published 20 November 2014)

We present an efficient method to extract the amount of true randomness that can be obtained by a quantum random number generator (QRNG). By repeating the measurements of a quantum system and by swapping between two mutually unbiased bases, a lower bound of the achievable true randomness can be evaluated. The bound is obtained thanks to the uncertainty principle of complementary measurements applied to min-entropy and max-entropy. We tested our method with two different QRNGs by using a train of qubits or ququart and demonstrated the scalability toward practical applications.

DOI: 10.1103/PhysRevA.90.052327 PACS number(s): 03.67.Dd, 03.65.−w, 05.40.−a, 42.50.Ex

I. INTRODUCTION

Random numbers are of fundamental importance for scientific and practical applications. Over the last years, great effort has been devoted to quantum random number generators (QRNGs), based on the intrinsic randomness of the quantum measurement process [1–10].

Theoretical analyses about the security and the real content of randomness have been given only recently [9–13]. It has been shown that *true random numbers*, i.e. uniform and uncorrelated from any classical or quantum side-information held by an eavesdropper, can be achieved by using the randomness *expansion* [13,14] or *amplification* protocols [7,15]. Expansion refers to a protocol able to generate true random numbers by starting with a short random seed. In an amplification protocol, the initial seed can have arbitrarily weak (but nonzero) randomness at the price of lower output rate. However, both protocols are very demanding under the experimental point of view since, by operating in the device-independent framework, the only way to get perfect randomness is to enforce conditions of nonlocality and nonsignalling between two parties that violate a (loophole-free) Bell inequality [9].

A general QRNG works as follows: given a d-level quantum system A prepared in a state ρ_A, the random variable Z is obtained by measuring the state ρ_A with a d-outcome measurement $\mathbb{Z}$: each outcome z is obtained with a given probability P_z. If the state ρ_A is pure, the number of true random bits that can be extracted from each measurement is quantified by the classical min-entropy $H_\infty(Z) = -\max_z(\log_2 P_z)$. In this work we aim to deal with a generic scenario, in which the state ρ_A is not pure and therefore the system A is correlated with another quantum system, denoted by E. In this case it is necessary to estimate the amount of (quantum) information that an adversary Eve holding the system E has on the variable Z. The importance of this estimation can be illustrated by a simple example. Let us suppose that Eve holds two entangled photons in the state $|\Phi\rangle = \frac{1}{\sqrt{2}}(|HH\rangle + |VV\rangle)$ and sends to Alice one of the two photons as the system she uses for the randomness extraction. If Alice measures in the $\{|H\rangle,|V\rangle\}$ basis she obtains a perfect random bit from the point of view of the classical min-entropy, since the two outcomes $|H\rangle$ and $|V\rangle$ are equally probable. However, due to the correlations in the $|\Phi\rangle$ state, Eve knows perfectly the outputs of Alice's measurements: the "random" bit held by Alice can be predicted with certainty by Eve.

The amount of true random bits that can be extracted from the random variable Z, if one requires uniformity and independence from the environment system E, is given by the conditional min-entropy $H_{\min}(Z|E)$ [16,17]. Indeed, the probability of guessing Z by holding the quantum system E is given by [18]

$$p_{\text{guess}}(Z|E) = 2^{-H_{\min}(Z|E)}. \tag{1}$$

For instance, in the previous example with the entangled state $|\Phi\rangle$, $p_{\text{guess}}(Z|E) = 1$ and the system held by Alice does not allow the generation of true random numbers.

We present a method, based on the uncertainty principle (UP), to estimate the conditional min-entropy and then the amount of true randomness that can be obtained by a given source. We show and experimentally test that, by measuring the system in conjugate observables $\mathbb{Z}$ and $\mathbb{X}$, it is possible to obtain the following bound on the conditional min-entropy:

$$H_{\min}(Z|E) \geqslant \log_2 d - H_{1/2}(X), \tag{2}$$

where d is the dimension of the Hilbert space and $H_{1/2}(X)$ is the max-entropy of $\mathbb{X}$ outcomes (see below). The measurement $\mathbb{Z}$ is used to generate the random sequence Z, while the measurement $\mathbb{X}$ is used to quantify the amount of true randomness contained in Z. In our protocol we do not use any assumption on the source ρ_A: an adversary, called Eve can have full control on the source and the environment E. The bound (2) is achieved by only assuming trusted a measurement device, meaning that Eve has no access to it and that the device performs a given positive-operator-value measure (POVM) that is only sensitive to a subspace of dimension d. To prevent the possibility that an adversary controls the detection efficiency, as reported in quantum hacking against detectors [19–21], it is necessary to monitor all detector parameters, such as bias voltage, current, and temperature [22]. The advantage of the method presented resides in its simplicity: no Bell inequality violation is required but it is only necessary to measure the system in two conjugate bases. With an initial seed of true randomness, our protocol is able to expand the randomness by taking into account all possible side quantum information possessed by Eve.

II. PROOF OF MAIN RESULT

In this section we derive our main result (2). We first start by reviewing the uncertainty relation for min- and max-conditional entropies introduced in Refs. [23–25].

A. Uncertainty principle

Let us consider three quantum systems A, B, and E, and let ρ_{ABE} be a tripartite state. Define $\mathbb{Z}$ and $\mathbb{X}$ as two POVMs on A with elements $\{\hat{\mathcal{M}}_z\}$ and $\{\hat{\mathcal{N}}_x\}$, and random outcomes Z and X encoded in two orthonormal bases $\{|z\rangle\}$ and $\{|x\rangle\}$. Then, the uncertainty principle is written as

$$H_{\min}(Z|E)_\rho + H_{\max}(X|B)_\rho \geqslant q, \tag{3}$$

where the min-entropy and max-entropy (see Appendix A and Ref. [18] for definitions of min-entropy and max-entropy) are evaluated on the postmeasurement states $\rho_{ZE} \equiv \sum_z |z\rangle\langle z| \otimes \mathrm{Tr}_{AB}[\hat{\mathcal{M}}_z \rho_{ABE}]$, $\rho_{XB} \equiv \sum_x |x\rangle\langle x| \otimes \mathrm{Tr}_{AE}[\hat{\mathcal{N}}_x \rho_{ABE}]$, and

$$q \equiv \log_2 \frac{1}{c}, \quad c \equiv \max_{z,x} \|\sqrt{\hat{\mathcal{M}}_z}\sqrt{\hat{\mathcal{N}}_x}\|_\infty^2. \tag{4}$$

The parameter c represents the maximum "overlap" between the two POVMs, and q quantifies the "incompatibility" of the measurements. If $\hat{\mathcal{M}}_z$ and $\hat{\mathcal{N}}_x$ are projective measurements corresponding to mutually unbiased bases in dimension d, then $c = \frac{1}{d}$.

B. Proof of bound

In a QRNG, Alice measures its system ρ_A by using a POVM measurement $\mathbb{Z} \equiv \{\hat{\mathcal{M}}_z\}$.[1] The state ρ_A is, in general, correlated with an external system E such that $\rho_A = \mathrm{Tr}_E[\rho_{AE}]$. The possible outcomes of the POVM can be encoded in an orthonormal basis $\{|z\rangle_A\}$, such that the postmeasurement state is $\rho_{ZE} \equiv \sum_z |z\rangle\langle z| \otimes \mathrm{Tr}_A[\hat{\mathcal{M}}_z \rho_{AE}] = \sum_z P_z |z\rangle\langle z| \otimes \rho_E^z$ with normalized ρ_E^z. Eve's knowledge about the possible outcomes of the $\mathbb{Z}$ measurements is given by the min-entropy $H_{\min}(Z|E)$, evaluated over ρ_{ZE}. If Alice sometimes measures her system with a different POVM $\mathbb{X}$, the UP allows us to bound the min-entropy $H_{\min}(Z|E)$ and then the guessing probability by Eq. (1). In fact, by using Eq. (3) and by considering the system B as a trivial space, the uncertainty relation becomes $H_{\min}(Z|E) \geqslant q - H_{\max}(X)$, where the max-entropy must be evaluated on the state obtained by the $\mathbb{X}$ measurement; namely, $\rho_X \equiv \sum_x p_x |x\rangle\langle x|$, with $p_x = \mathrm{Tr}_{AE}[\hat{\mathcal{N}}_x \rho_{AE}]$. In this case $H_{\max}(X) = 2\log_2 \mathrm{Tr}[\sqrt{\rho_X}]$ (see Appendix A and Ref. [18]), i.e., the max-entropy is equal to $H_{1/2}(X)$, the Rényi entropy[2] of order $1/2$ of the classical outcome X.

Our result can be summarized as follows: the conditional min-entropy of the $\mathbb{Z}$ outputs can be bounded by using the Rényi entropy of order $1/2$ of the $\mathbb{X}$ outputs; namely,

$$H_{\min}(Z|E) \geqslant q - H_{1/2}(X), \tag{5}$$

which reduces to Eq. (2) in case of conjugate observables in d dimensions. We would like to point out that, thanks to the inequality $H_{1/2}(X) + H_\infty(Z) \geqslant q$ derived by Maassen and Uffink [26], the bound $q - H_{1/2}(X)$ is always lower than the classical min-entropy $H_\infty(Z)$ evaluated on the probabilities P_z.

III. UP-CERTIFIED QUANTUM RANDOM-NUMBER GENERATOR

Let us now evaluate the bound in two particular cases. Let us consider the $\mathbb{Z}$ POVM as projective measurements in the computational basis, $\{|0\rangle, |1\rangle, \ldots, |d-1\rangle\}$, and let the $\mathbb{X}$ measurement be chosen as its discrete-Fourier transform $|x\rangle = \frac{1}{\sqrt{d}} \sum_{z=0}^{d-1} e^{i\frac{xz}{2\pi d}} |z\rangle$ for which $q = \log_2 d$. If the system A is prepared in the state $|\psi\rangle_A = \frac{1}{\sqrt{d}} \sum_z |z\rangle$, then $H_{1/2}(X) = 0$ and Eq. (5) bounds $H_{\min}(Z|E)$ to the classical min-entropy $H_\infty(Z) = \log_2 d$. The random variable Z is then uniformly distributed and independent of any adversary. However, in practical implementations of a QRNG, it is impossible to prepare the system A in a perfect pure state $|\psi\rangle_A$. When the state ρ_A is not pure, the entropies $H_\infty(Z)$ and $H_{\min}(Z|E)$ can be different. Our result is thus particularly effective with real sources (that cannot generate pure states) since it bounds the effective achievable randomness without requiring any assumption on them. Even if Eve has complete control over the source ρ_A, the bound given in Eq. (5) evaluates the amount of true random bits that can extracted from Z. This randomness has complete quantum origin and no side information can be used to predict the generated random bits.

Another important example is represented by the system described in the introduction: Eve sends to Alice one photon of a two-photon maximally entangled state and thus can perfectly predict the outputs of Alice's measurements. In this case, Alice holds a completely mixed state $\rho_A = \frac{1}{2}\mathbb{1}_2$ and the max-entropy is $H_{1/2}(X) = 1$. Thanks to Eqs. (5) and (1), the bound on the min-entropy becomes trivial, $H_{\min}(Z|E) \geqslant 0$ and $p_{\mathrm{guess}}(Z|E) \leqslant 1$: our result correctly predicts that the guessing probability can reach unity and so no true random bits can be extracted in this case.

In order to exploit the result of Eq. (5) it is necessary to estimate the max-entropy of the source $\rho_A = \mathrm{Tr}_E[\rho_{AE}]$. However, since the POVM $\{\hat{\mathcal{M}}_z\}$ and $\{\hat{\mathcal{N}}_x\}$ are incompatible, it is not possible to measure them at the same time. We then need to switch randomly between $\hat{\mathcal{M}}_z$ and $\hat{\mathcal{N}}_x$ during the random bit generation (see Fig. 1). The measurements are chosen by using a seed of true randomness that our method is able to expand. From this point of view, our method can be seen as a random-number expansion protocol.

We now show that the number of random extracted bits is greater than the required seed. Let m be the total number of measurements. We decide that, over m, the number of measurements in the POVM $\{\hat{\mathcal{N}}_x\}$ will be $n_X = \lceil\sqrt{m}\rceil$, such that the probability of measuring in the $\mathbb{X}$ basis is approximately $\frac{1}{\sqrt{m}}$. To randomly choose n_X among m measurements we need a number of bits given by $t(m) = \lceil \log_2 \frac{m!}{n_X!(m-n_X)!} \rceil$. This is the length of the random seed required for the randomness expansion.

[1] We employed POVMs to present our method in a general framework, but projective measurements are more suited for practical applications.

[2] We recall that the Rényi entropy of order α is defined as $H_\alpha(X) = \frac{1}{1-\alpha} \log_2 \sum_{x=0}^{d-1} p_x^\alpha$.

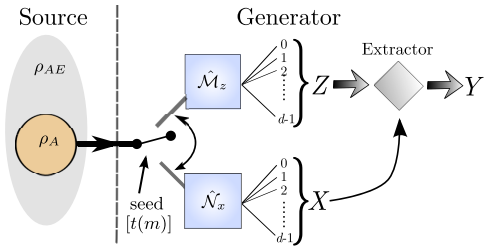

FIG. 1. (Color online) Scheme of the QRNG. The source of randomness is the state ρ_A that can be correlated with a larger system E. An initial perfect random seed of length $t(m)$ is used to switch between the $\{\hat{\mathcal{M}}_z\}$ and $\{\hat{\mathcal{N}}_x\}$ POVMs, from which the random variables Z and X are extracted. The variable Z is used to generate the random sequence, while the variable X is used to evaluate how many true random bits can be extracted by Z. Y represents the final true random sequence.

The outcome probabilities in the $\mathbb{X}$ basis are given by $p_x = \mathrm{Tr}_A[\hat{\mathcal{N}}_x \rho_A]$ and the asymptotic lower bound of the min-entropy is $H_{\min}(Z|E) \geqslant q - H_{1/2}(X)$. From the experimental point of view we need to estimate the max-entropy $H_{1/2}(X)$ by using the n_X outcomes. If we denote by n_x the number of outcomes such that $X = x$, we can estimate the max-entropy by using the Bayesian estimator defined in Ref. [27] (with a uniform prior distribution):

$$\widetilde{H}_{1/2}(\{n_x\}) = 2\log_2\left[\frac{\Gamma(n_X+d)}{\Gamma\left(n_X+d+\frac{1}{2}\right)}\sum_{x=0}^{d-1}\frac{\Gamma\left(n_x+\frac{3}{2}\right)}{\Gamma(n_x+1)}\right]. \tag{6}$$

The Bayesian estimator has a lower variance with respect to the frequentist estimator $\widetilde{H}^f_{1/2} = 2\log_2[\sum_{x=0}^{d-1}(\frac{n_x}{n_X})^{1/2}]$. Moreover, for low max-entropies, the frequentist estimator has a negative bias that overestimates the bound on the min-entropy.

Then, given m measurements, the number of extracted random bits are the outputs of the $\mathbb{Z}$ measurement, given by $m - n_X$: due to the bound (5), at least $(m - n_X)[q - H_{1/2}(X)]$ are true random bits. If we subtract the number of bits $t(m)$ required for the seed, we can estimate the random bits' generation rate per measurement as

$$\widetilde{r}(\{n_x\}) = \frac{b_{\mathrm{sec}}}{m}, \tag{7}$$

where b_{sec} is the number of generated true random bits :

$$b_{\mathrm{sec}} = (m - n_X)[q - \widetilde{H}_{\max}(\{n_x\})] - t(m). \tag{8}$$

It is worth noticing that, in the infinite-size limit $m \to +\infty$, the seed length is given by $t(m) \sim \sqrt{m}\log_2\sqrt{m}$, the estimator $\widetilde{H}_{1/2}(\{n_x\}) \sim H_{1/2}(X)$, and the rate approaches the asymptotic limit $\widetilde{r} \longrightarrow r(Z) = q - H_{1/2}(X)$. Since the number of extracted random bits are quadratically larger than the initial seed bits, the generator can work in loop: an initial seed is expanded and part of the extracted randomness is fed in as a new seed.

IV. EXPERIMENTAL REALIZATION

We experimentally tested our method with two different random-number generators implemented by photon pairs

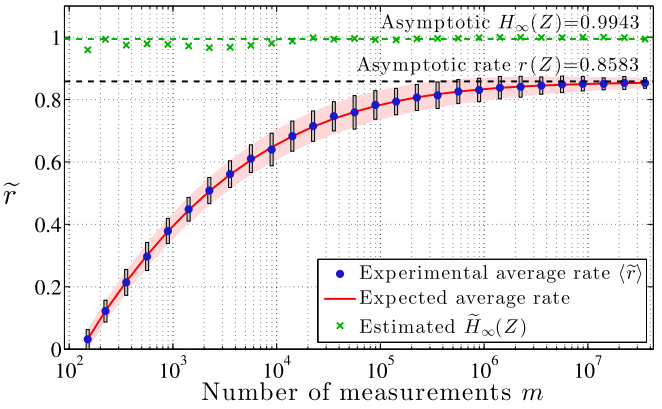

FIG. 2. (Color online) Average experimental rate for the qubit QRNG. Blue circles represent the experimental average rate $\widetilde{r}$ of true random bits per measurement, while the continuous red line is the theoretical prediction with $\rho_X = \sum_{x=0}^{1} p_x|x\rangle\langle x|$ where $p_0 = 0.9973$ and $p_1 = 0.0027$. The shaded red area represents the theoretical standard deviation of the rate, while gray rectangles show the experimental standard deviation of the rate. Green crosses show the classical min-entropy estimated on the Z random variable. The asymptotic limit $H_\infty(Z)$ is evaluated on the state $\rho_Z = \sum_{z=0}^{1} P_z|z\rangle\langle z|$ with $P_0 = 0.5020$ and $P_1 = 0.4980$.

generated in the $|HV\rangle$ state by spontaneous parametric down conversion. See Appendix B for details about the source. The first generator is a single qubit QRNG operated by a heralded single-photon source: one photon of the pair, measured in the $|H\rangle$ state, is used as trigger, while the second represents the signal. By measuring the signal photon in the $\mathbb{Z} = \{|+\rangle, |-\rangle\}$ and $\mathbb{X} = \{|H\rangle, |V\rangle\}$ bases, we generate the random variables Z and X. Here we denote with $|\pm\rangle$ the diagonal polarization states $\frac{1}{\sqrt{2}}(|H\rangle \pm |V\rangle)$. The second generator is a four-level system (ququart) QRNG, represented by the pair of photons. In this case the $\mathbb{Z}$ and $\mathbb{X}$ bases are respectively given by $\{|{+}{+}\rangle, |{+}{-}\rangle, |{-}{+}\rangle, |{-}{-}\rangle\}$ and $\{|HV\rangle, |VV\rangle, |HH\rangle, |VH\rangle\}$.

We first analyze the qubit QRNG. By choosing different values of m we performed $n_X = \lceil\sqrt{m}\rceil$ measurements in the $\mathbb{X}$ basis and $n_Z = m - n_X$ measurements in the $\mathbb{Z}$ basis, obtaining the sequences X and Z. The two sequences are used to estimate the classical max-entropy $\widetilde{H}_{1/2}(\{n_x\})$ and the rate $\widetilde{r}(\{n_x\})$. For each m, in Fig. 2 we show the average rate $\widetilde{r}$ and its standard deviation experimentally evaluated over 200 different X sequences of n_X bits (see Appendix C for the rate achieved, for each m, by a single X sequence of n_X bits). The experimental rates can be compared with the predicted average rate $\langle\widetilde{r}\rangle = \sum_{\{n_x\}}\Pi(\{n_x\})\widetilde{r}(\{n_x\})$, obtained by averaging $\widetilde{r}(\{n_x\})$ over the multinomial distribution

$$\Pi(\{n_x\}) = \frac{n_X!}{n_0!n_1!\cdots n_{d-1}!}p_0^{n_0}p_1^{n_1}\cdots p_{d-1}^{n_{d-1}}.$$

We also show the classical min-entropy $\widetilde{H}_\infty(Z)$ evaluated on a sequence Z with n_Z bits. The figure shows very good agreement between the experimental result and the theoretical prediction. It is worth noticing that at least $m > 150$ measurements are necessary to obtain a positive rate $\widetilde{r}$, while with just $m \simeq 10^6$ the rate is very close to the asymptotic bound $r(Z)$. The difference between $H_\infty(Z)$ and $\widetilde{r}$ corresponds to the

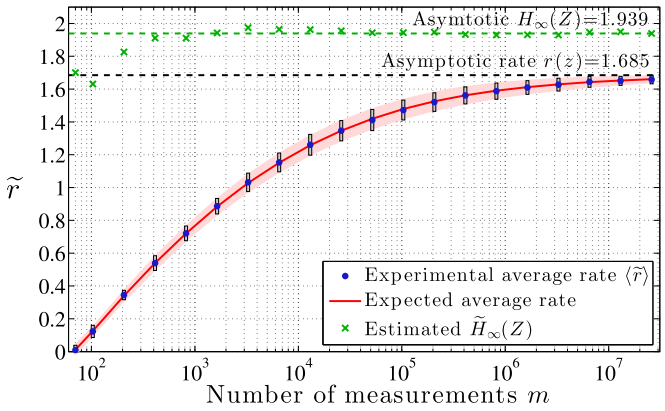

FIG. 3. (Color online) Average experimental rate for the ququart QRNG. See Fig. 2 for notations. In this case $\rho_X = \sum_{x=0}^{3} p_x |x\rangle\langle x|$ with $p_0 = 0.9937$, $p_1 = 0.003\,59$, $p_2 = 0.002\,66$, and $p_3 = 1 - p_0 - p_1 - p_2$ and $\rho_Z = \sum_{z=0}^{3} P_z |z\rangle\langle z|$ with $P_0 = 0.2527$, $P_1 = 0.2412$, $P_2 = 0.2608$, and $P_3 = 0.2453$.

possible knowledge that may have an adversary holding the system E. The limit $H_\infty(Z)$ is often and erroneously taken as the amount of true randomness used to calibrate the extractor: in this way, even if the output string appears statistically good, possible side information held by Eve is not completely erased. In our experimental analysis, since we are mainly interested in demonstrating the physical principles, we did not use active switches to change between the two bases (we first measured the Z sequence and afterwards the X sequence). For practical applications, however, the QRNG should contain an active switch controlled by the seed $t(m)$.

In Fig. 3 the results for the ququart QRNG are presented. Also in this case, for each m, the average rate $\tilde{r}$ and its standard deviation are experimentally obtained by 200 different X sequences of $n_X(m)$ bits. Again, there is a very good agreement between the experimental results and the theoretical predictions and a positive (average) rate is obtained for $m > 70$. As before, for $m \simeq 10^6$ the rate is very close to the asymptotic bound $r(Z)$: thanks to the larger Hilbert space, we can asymptotically obtain 1.685 bits per measurement, which should be compared with the value 0.8583 achieved with the qubit QRNG. Our method is thus very robust with respect to the increasing of the dimension d of the system.

For the complete proof of our protocol, we performed the extraction on a long random sequence Z, and the results are presented in Appendix D.

Detailed comparison with Ref. [2]

Here we give a detailed comparison between our method and the result of Fiorentino *et al.* [2], where the conditional min-entropy of a qubit state is evaluated by measuring its density matrix $\rho = \frac{1}{2}(\mathbb{1} + \vec{r}\cdot\vec{\sigma})$ (σ_i are the Pauli matrices and $\vec{r}$ is a three-dimensional vector such that $|\vec{r}| \leqslant 1$). By extracting the random bits by measuring the qubit in the computational basis $\mathbb{Z} = \{|0\rangle, |1\rangle\}$ such that $r_z = \langle 0|\rho|0\rangle - \langle 1|\rho|1\rangle$, the conditional min-entropy was estimated to be $H_{\min}(Z|E) = 1 - \log_2[1 + (1 - r_x^2 - r_y^2)^{1/2}]$ [2].

Our method estimates the min-entropy of the Z outcomes by measuring in the $\mathbb{X} = \{|\pm\rangle\}$ basis giving the asymptotic bound of $H_{\min}(Z|E) \geqslant 1 - \log_2[1 + (1 - r_x^2)^{1/2}]$. Our result is a lower bound, since $q - H_{1/2}(X) = 1 - \log_2[1 + (1 - r_x^2)^{1/2}]$: the bound is tight when $r_y = 0$. If the state is pure, the result of Ref. [2] allows to achieve the upper limit $H_{\min}(Z|E) = H_\infty(Z)$. The advantage of our approach resides in the fact that it is not necessary to measure the full density matrix but only measurements on two mutually unbiased bases. Indeed, in order to evaluate the density matrix, it is necessary to measure the system also in the $\mathbb{X}$ and $\mathbb{Y} = \{\frac{1}{\sqrt{2}}(|0\rangle \pm i|1\rangle)\}$ basis beside the basis chosen to obtain the random sequence. Also in the case of Ref. [2], a random seed is needed to switch between the tomography bases and the random sequence basis. As a final consideration, the result of Fiorentino *et al.* applies only to qubit systems, while our result can be applied to a general qudit systems, as we have demonstrated by analyzing the ququart QRNG.

We now give a detailed comparison for finite m: let us consider the following parameters $r_z = 0.9947 \pm 0.001$ and $r_x = 0.004 \pm 0.002$ corresponding to the experimental measured parameter of our qubit QRNG. Since the norm of the vector $\vec{r}$ cannot be greater that 1, it implies that $|r_y| \leqslant (1 - r_z^2 - r_x^2)^{1/2} \leqslant 0.1027$, corresponding to a purity greater that $\mathcal{P}_{\min} = 0.9947$. We recall that purity of the state ρ is defined as $\mathcal{P} = \mathrm{Tr}[\rho^2] = \frac{1}{2}(1 + r_x^2 + r_y^2 + r_z^2)$. The measurement in the Y basis will allow us to determine the r_y parameter.

We performed the detailed comparison in the finite-m case (m is the total number of measurements) between our method and Ref. [2]. To obtain a fair comparison we set $n_X^* = n_Y^* = \lceil\sqrt{m}/2\rceil$ as the number of measurements in the X and Y bases, respectively, for the tomographic method of Ref. [2]. Then the number of measurements in the Z basis is given by $n_Z^* = m - 2\lceil\sqrt{m}/2\rceil$. From such measurements the r_x and r_y parameters are estimated as (we used Bayesian estimators):

$$r_x = \frac{n_{0x} - n_{1x}}{n_{0x} + n_{1x} + 2}, \quad r_y = \frac{n_{0y} - n_{1y}}{n_{0y} + n_{1y} + 2}. \tag{9}$$

To randomly choose the X and Y measurements over the total number of measurements m we need a number of bits given by

$$t^*(m) = 2\left\lceil \log_2 \frac{m!}{(2n_X^*)!(m - 2n_X^*)!} \right\rceil.$$

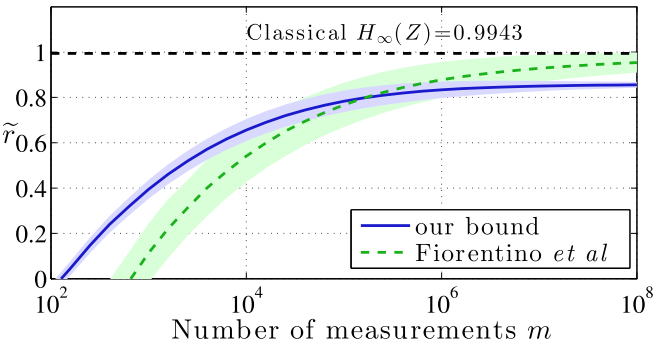

FIG. 4. (Color online) Comparison between the rate achievable by our bound (continuous blue line) and the rate achievable with the min-entropy estimation of Ref. [2] (dotted green line) in the case of perfect pure state with purity $\mathcal{P} = 1$.

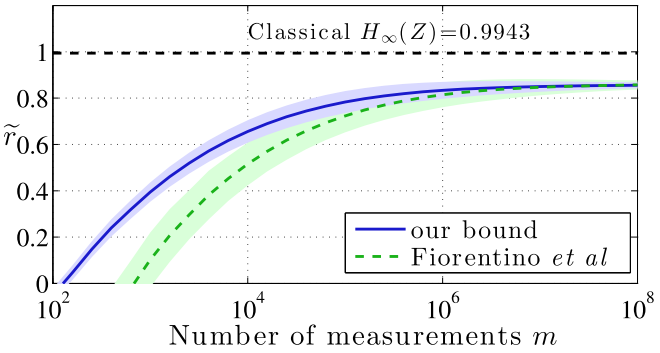

FIG. 5. (Color online) Comparison between the rate achievable by our bound (continuous blue line) and the rate achievable with the min-entropy estimation of Ref. [2] (dotted green line) in the case of slightly mixed state with purity $\mathcal{P} = 0.995$.

In Figs. 4 and 5 we show the comparison between the two rates in the case of a perfect pure state $\mathcal{P} = 1$ and in the case of $r_y = 0$, corresponding to $\mathcal{P} = 0.995$: the figures show that our results are slightly outperformed by the tomographic extractor only for high-purity states $\mathcal{P} > 0.995$ and in the large-m regime ($m > 10^5$). A maximum of 15% improvement with respect to the results shown in Fig. 2 is expected if the generated state is pure $\mathcal{P} = 1$ and $N > 10^8$. However, to obtain such limited advantage, a complication in the scheme; namely, the measurement in the Y basis, is required.

V. CONCLUSIONS

We provided a bound, given by Eq. (5), to directly compute the conditional min-entropy $H_{\min}(Z|E)$ of the random variable Z, by using the classical random variable X. The variables Z and X are obtained by measuring the system in two mutually unbiased bases. $H_{\min}(Z|E)$ represents the amount of true randomness that can be extracted from Z. No assumption is made on the source and/or the dimension of Hilbert space. Our result is based on the fact the measurement device is trusted: we assumed that the measurement system (wave plates and polarizing beam splitters) works properly and the detector efficiency is not dependent on the input state or on an external control. In order for the detection system to be only sensitive to a well-known and characterized finite-dimensional subspace of the total Hilbert space, photon-number-resolving detectors or the squashing model of quantum key distribution [28,29] can be implemented. It is important to stress that, if the source does not generate a perfect pure state (and this always happens in experimental realizations), the randomness extracted by standard methods; namely, by measuring the system in a single basis, is not a true randomness: an eavesdropper can have (partial or full) information about the generated random bits. We also tested our bound with a qubit and a ququart QRNG with good agreement between theory and experiment.

Our method can be extended by taking into account possible imperfections in the measurement device, as illustrated in Ref. [16]. We believe that our method can be very useful for the extraction of true randomness and can be applied in the framework of practical high-speed QRNGs [6,8], since it guarantees protection against quantum side information without the need of a complex Bell-violation experiment.

ACKNOWLEDGMENTS

We would like to thank Alberto Dall'Arche of the University of Padova for his support on the setup preparation. Our work was supported by the Strategic-Research-Project QUINTET of the Department of Information Engineering, University of Padova and the Strategic-Research-Project QUANTUMFUTURE (STPD08ZXSJ) of the University of Padova.

APPENDIX A: MIN-ENTROPY AND MAX-ENTROPY

We here briefly review the definition of conditional min-entropy and max-entropy introduced in Ref. [18]. The conditional min-entropy of a bipartite quantum state ρ_{AE} is defined as

$$H_{\min}(A|E)_{\rho_{AE}} = \max_{\sigma_B} \sup \left\{ \lambda \in \mathbb{R} \left| \frac{\mathbb{1}_A \otimes \sigma_E}{2^\lambda} \geqslant \rho_{AE} \right. \right\}, \quad \text{(A1)}$$

where σ_E is a normalized positive state.

The conditional max-entropy is the dual of the min-entropy. In fact, by using a purification ρ_{ABC} of ρ_{AB}, the max-entropy is defined by

$$H_{\max}(A|B)_{\rho_{AB}} = -H_{\min}(A|C)_{\rho_{AC}}, \quad \text{(A2)}$$

where $\rho_{AB} = \mathrm{Tr}_C[\rho_{ABC}]$ and $\rho_{AC} = \mathrm{Tr}_B[\rho_{ABC}]$. We recall here that the purification of a state ρ_{AB} is a pure state ρ_{ABC} in the extended Hilbert space $A \otimes B \otimes C$, such that $\mathrm{Tr}_C[\rho_{ABC}] = \rho_{AB}$.

For the QRNG we need to evaluate the max-entropy for the state $\rho_X \equiv \sum_{x=0}^{d-1} p_x |x\rangle\langle x|$, where the space B is a trivial space. By definition (A2) we have

$$H_{\max}(X)_{\rho_X} = -H_{\min}(A|C)_{\rho_{AC}}, \quad \text{(A3)}$$

with ρ_{AC} being a purification of ρ_X. A possible purification is given by

$$\rho_{AC} = |\Psi\rangle_{AC}\langle\Psi|, \quad |\Psi\rangle_{AC} = \sum_{x=0}^{d-1} \sqrt{p_x} |x\rangle_A \otimes |v_x\rangle_C, \quad \text{(A4)}$$

with $\{|v_x\rangle\}$ on the orthonormal basis on the space C with dimension d. By Eq. (A1) we have

$$\begin{aligned} H_{\max}(X)_{\rho_X} &= -H_{\min}(A|C)_{\rho_{AC}} \\ &= -\max_{\sigma_B} \sup \left\{ \lambda \in \mathbb{R} \left| \frac{\mathbb{1}_A \otimes \sigma_C}{2^\lambda} \geqslant |\Psi\rangle\langle\Psi| \right. \right\}. \end{aligned} \quad \text{(A5)}$$

The state σ_C that maximizes the min-entropy definition is $\sigma_C = \mathbb{1}/d$. The maximum λ such that $\mathbb{1}_A \otimes \mathbb{1}_C \geqslant d2^\lambda |\Psi\rangle\langle\Psi|$ is $\lambda = -\log_2[\sum_x (\sqrt{p_x})]^2$, such that

$$H_{\max}(X)_{\rho_X} = \log_2 \left[\sum_x \sqrt{p_x} \right]^2 = 2 \log_2 \sum_x \sqrt{p_x} = H_{1/2}(X). \quad \text{(A6)}$$

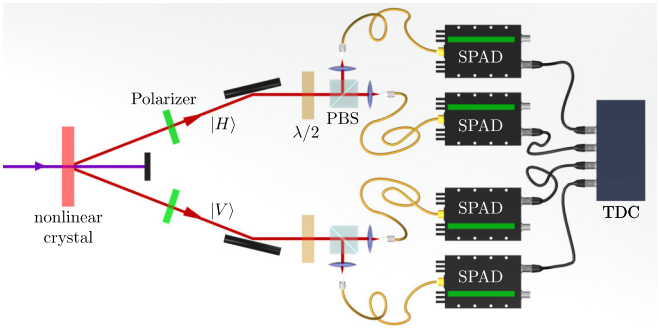

FIG. 6. (Color online) Scheme of experimental setup generating the SPDC photons. TDC is time-to-digital converter, SPAD is single-photon avalanche diode, PBS is polarizing beam splitter, $\lambda/2$ are wave plates.

APPENDIX B: PHOTON SOURCE

Photons used in experimental demonstration of the method were generated by spontaneous parametric down conversion (SPDC), as illustrated in Fig. 6. A femtosecond pulsed laser (76 MHz repetition rate) at 405 nm shines on a nonlinear crystal where pairs of photons are probabilistically emitted over two correlated directions. Two polarizers select the $|HV\rangle$ pair, with $|H\rangle$ and $|V\rangle$ being the horizontal and vertical polarized photon, respectively. Half-wave plates $\lambda/2$ allow us to change between the $\mathbb{Z}$ and $\mathbb{X}$ bases. For the single qubit QRNG, the $|H\rangle$ photon is used as a trigger: its detection heralds the presence of the $|V\rangle$ photon. Single-photon detectors (SPADs) deliver signals to a time-to-digital converter (TDC). Concerning the rate of raw-bit extraction, the source has a coincidence rate of 12 kHz: we would like to point out that we are not interested in the speed of the generator, but on the demonstration of the method presented here. However, it is worth noticing that sources producing photon pairs at the rate of few MHz are currently available [30,31].

APPENDIX C: ANALYSIS OF RANDOM-BIT GENERATION RATE

In this Appendix we show the experimental rate obtained with a single control X sequence, while in the main text we showed the average value obtained with 200 sequences. We report the rate achieved with the qubit QRNG. We recall here that, given m measurements on the state ρ_A, we obtained two classical X and Z sequences with n_X and n_Z bits, respectively, whose lengths are respectively given by $n_X = \lceil \sqrt{m} \rceil$ and $n_Z = m - n_X$. The state of the system A after the measurement is given by $\rho_Z = \sum_{z=0}^{1} P_z |z\rangle\langle z|$ or $\rho_X = \sum_{x=0}^{1} p_x |x\rangle\langle x|$, depending on the POVM used.

Given m, we would like to evaluate the "single-shot" rate $\widetilde{r}$ given by

$$\widetilde{r}(n_0,n_1,m) = (m - n_X)[1 - \widetilde{H}_{1/2}(n_0,n_1)] - t(m), \qquad \text{(C1)}$$

with n_0 and n_1 being the number of zeros and ones in the X sequence.

For the single-qubit QRNG, since $n_0 + n_1 = n_X$, the single-shot rate is a function of only m and n_1:

$$\widetilde{r}(n_1,m) = (m - n_X)\left\{1 - 2\log_2\left[\frac{\Gamma(n_X+2)}{\Gamma\left(n_X+\frac{5}{2}\right)}\right] - 2\log_2\left[\frac{\Gamma\left(n_X - n_1 + \frac{3}{2}\right)}{\Gamma(n_X - n_1 + 1)} + \frac{\Gamma\left(n_1+\frac{3}{2}\right)}{\Gamma(n_1+1)}\right]\right\} - \left\lceil \log_2 \binom{m}{n_X} \right\rceil. \qquad \text{(C2)}$$

For different values of m we show in Fig. 7 the achieved rate: each point represents the rate $\widetilde{r}$ evaluated over a single X sequence of n_X bits obtained by the measurement in the $\mathbb{X}$ POVM. Each sequence is taken from a sample with the following property:

$$\rho_X = \sum_{x=0}^{1} p_x |x\rangle\langle x| \text{ with } p_0 = 0.9973, \quad p_1 = 0.0027. \qquad \text{(C3)}$$

For perfect-state preparation we would like to have $p_0 = 1$ and $p_1 = 0$: by this reason, the number of ones in the X sequence are defined as the "number of errors" in the sequence. The errors can be caused by the presence of the eavesdropper, or by imperfections in the preparation devices. Since p_1 is very low, in Fig. 7 it is possible to see that, for $m < 10^3$, few sequences have 1 errors and the most have 0 errors. By increasing m, the number of errors increases to follow the prediction $n_1 \sim p_1 n_X$. For low m, the possible rates are "quantized," since the rate is evaluated on integer values n_0 and n_1. In Fig. 8 we show estimated max-entropy $\widetilde{H}_{1/2}(X)$ as a function of the number of errors for the case $n_X = 100$ and $n_X = 1000$. We also report the probability of obtaining n_1 errors, given by $\Pi(n_1) = \binom{n_X}{n_1} p_0^{n_0} p_1^{n_1}$. The figure shows that

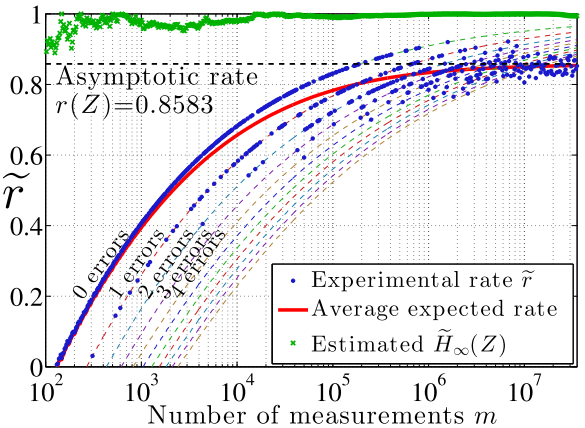

FIG. 7. (Color online) Experimental rate for the qubit RNG. Blue circles represent the experimental rate $\widetilde{r}$ of true random bits per measurement, while continuous red line represents the theoretical average prediction with $\rho_X = \sum_{x=0}^{1} p_x |x\rangle\langle x|$ where $p_0 = 0.9973$ and $p_1 = 0.0027$. Dashed lines represent the rate achieved with different numbers of "errors" in the X sequence. Green crosses show the classical min-entropy estimated on the Z random variable obtained from the state $\rho_Z = \sum_{z=0}^{1} P_z |z\rangle\langle z|$ with $P_0 = 0.5020$ and $P_1 = 0.4980$.

TABLE I. (Color online) (left column) Summary of the results of selected tests of batteries particularly effective in detecting defects in true random-number generator (TRNG). The *Alphabit* and *Rabbit* batteries belong to the TESTU01: critical results are if $\mathcal{P} \leqslant 10^{-3}$ or $\mathcal{P} \geqslant 0.990$. For tests which give more than a $\mathcal{P}$ values, the smallest is reported. For the NIST SP-800-22 suite, the file was partitioned in substrings 200 000 bits long for a total of 150 strings: this length was chosen in order to obtain a sample size sufficiently large such that it is likely to fail the tests in the case of poor randomness with a significance level of $\alpha = 0.01$; a test is failed if more than six strings fail it. In addition, a test is passed if the a χ-squared test on the distribution of $\mathcal{P}$ values, gives itself a $\mathcal{P}$ value $\mathcal{P} \geqslant 10^{-5}$. (right column) Summary of the results of selected tests of batteries particularly effective in detecting defects in TRNG. The *Alphabit* and *Rabbit* batteries belong to the TESTU01: critical results are if $\mathcal{P} \leqslant 10^{-3}$ or $\mathcal{P} \geqslant 0.990$. For tests which give more than a $\mathcal{P}$ values, the smallest is reported. For the NIST SP-800-22 suite, the file was partitioned in substrings 400 000 bits long for a total of 100 strings: this length was chosen in order to obtain a sample sizes sufficiently large such that it is likely to fail the tests in case of poor randomness with a significance level of $\alpha = 0.01$; a test is failed if more than four strings fail it. In addition, a test is passed if the a χ-squared test on the distribution of $\mathcal{P}$ values, gives itself a $\mathcal{P}$ value $\mathcal{P} \geqslant 10^{-5}$.

Suite	Test	P-Value	Suite	Test	P-Value
Rabbit	MultinomialBitsOver	0.94	Alphabit	MultinomialBitsOver (L = 2)	0.72
	ClosePairsBitMatch (t=2)	0.10		MultinomialBitsOver (L = 4)	0.38
	ClosePairsBitMatch (t=4)	0.10		MultinomialBitsOver (L = 8)	0.81
	AppearanceSpacings	0.76		MultinomialBitsOver (L = 16)	0.38
	LinearComp	0.23		HammingIndep (L = 16)	0.02
	LempelZiv	0.32		HammingIndep (L = 32)	0.64
	Fourier1	0.60		HammingCorr (L = 32)	0.72
	Fourier3	0.53		RandomWalk1 (L = 64)	0.04
	LongestHeadRun	0.59		RandomWalk1 (L = 320)	0.03
	PeriodsInStrings	0.950	SP-800-22	Test	P-Val. / Pass Ratio
	HammingWeight (L = 32)	0.24		Frequency	0.066882 / 149/150
	HammingCorr (L = 32)	0.72		BlockFrequency	0.299251 / 148/150
	HammingCorr (L = 64)	0.65		CumulativeSums	0.431143 / 149/150
	HammingCorr (L =128)	0.54		CumulativeSums	0.588652 / 148/150
	HammingIndep (L = 16)	0.02		Runs	0.671779 / 150/150
	HammingIndep (L = 32)	0.64		LongestRun	0.911413 / 149/150
	HammingIndep (L = 64)	0.89		Rank	0.132132 / 149/150
	AutoCor with a lag d = 1.	0.79		FFT	0.142602 / 148/150
	AutoCor with a lag d = 2.	0.86		NonOverlappingTemplate	148/148 (subtests)
	Run	0.20		OverlappingTemplate	0.056546 / 150/150
	MatrixRank (32 × 32)	0.56		ApproximateEntropy	0.520767 / 148/150
	RandomWalk1 (L = 128)	0.12		RandomExcursion	26/26 (subtests)
	RandomWalk1 (L = 1024)	0.12		Serial (M=16)	0.712961 / 149/150
	RandomWalk1 (L = 10016)	0.01		Serial (M=16)	0.236810 / 150/150
				LinearComplexity	0.092784 / 148/150

Suite	Test	P-Value	Suite	Test	P-Value
Rabbit	MultinomialBitsOver	0.27	Alphabit	MultinomialBitsOver (L = 2)	0.19
	ClosePairsBitMatch (t=2)	0.20		MultinomialBitsOver (L = 4)	0.23
	ClosePairsBitMatch (t=4)	0.58		MultinomialBitsOver (L = 8)	0.64
	AppearanceSpacings	0.67		MultinomialBitsOver (L = 16)	0.94
	LinearComp	0.19		HammingIndep (L = 16)	0.73
	LempelZiv	0.84		HammingIndep (L = 32)	0.73
	Fourier1	0.50		HammingCorr (L = 32)	0.52
	Fourier3	0.38		RandomWalk1 (L = 64)	0.29
	LongestHeadRun	0.04		RandomWalk1 (L = 320)	0.15
	PeriodsInStrings	0.37	SP-800-22	Test	P-Val. / Pass Ratio
	HammingWeight (L = 32)	0.51		Frequency	0.759756 / 97/100
	HammingCorr (L = 32)	0.52		BlockFrequency	0.964295 / 100/100
	HammingCorr (L = 64)	0.70		CumulativeSums	0.096578 / 97/100
	HammingCorr (L =128)	0.13		CumulativeSums	0.911413 / 97/100
	HammingIndep (L = 16)	0.73		Runs	0.779188 / 98/100
	HammingIndep (L = 32)	0.73		LongestRun	0.494392 / 99/100
	HammingIndep (L = 64)	0.71		Rank	0.011791 / 100/100
	AutoCor with a lag d = 1.	0.36		FFT	0.657933 / 100/100
	AutoCor with a lag d = 2.	0.26		NonOverlappingTemplate	148/148 (subtests)
	Run	0.02		OverlappingTemplate	0.816537 / 99/100
	MatrixRank (32 × 32)	0.39		Universal	0.289667 / 99/100
	MatrixRank (320 × 320)	0.84		ApproximateEntropy	0.867692 / 100/100
	RandomWalk1 (L = 128)	0.21		RandomExcursion	26/26 (subtests)
	RandomWalk1 (L = 1024)	0.51		Serial (M=16)	0.798139 / 98/100
	RandomWalk1 (L = 10016)	0.24		Serial (M=16)	0.514124 / 99/100
				LinearComplexity	0.401199 / 100/100

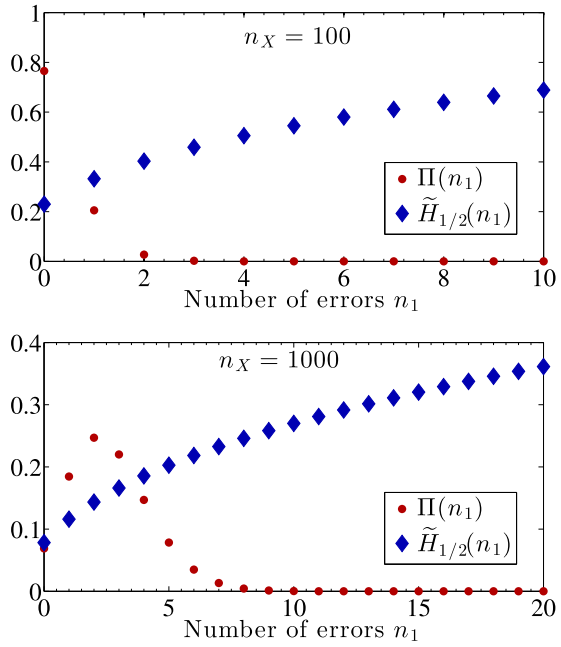

FIG. 8. (Color online) Estimated max-entropy $\widetilde{H}_{1/2}(X)$ and error probability $\Pi(n_1)$. Due to the low value of $p_1 = 0.0027$, the $\Pi(n_1)$ is peaked around the low values of n_1.

$\widetilde{H}_{1/2}(X)$ has discrete values corresponding to different values of n_1.

APPENDIX D: TESTS ON EXTRACTED RANDOM NUMBERS

As a quantitative example for the complete proof of our method, we performed the extraction on a long random sequence Z. For the qubit case we use a random sequence Z of length $n_Z = 35.6 \times 10^6$ and a control sequence X of length $n_X = 5967$, requiring a seed length $t(m) = 83\,443$. The estimated lower bound for the min-entropy is $1 - H_{1/2}(X) \simeq 0.8437$ giving an output random sequence Y of $b_{\text{sec}} \simeq 29.951 \times 10^6$ bits. For the qudit case, we have $n_Z = 25.770 \times 10^6$ and $n_X = 5100$ with a seed length $t(m) = 70\,163$. The estimated lower bound for the min-entropy is 1.690, giving $b_{\text{sec}} \simeq 43.886 \times 10^6$ true random bits. In both cases, the initial Z strings are fed to an extractor by two-universal hashing [16,32] to obtain the Y strings. As we now show, the obtained bits pass successfully the most stringent tests [33] for the assessment of the independent and identically distributed (i.i.d.) hypothesis for random bits.

At the present time, TEST-U01 [34] is the most stringent and comprehensive suite of tests; among all, we chose the pair sub-batteries *Rabbit* and *Alphabit*, respectively, specifically designed to tests RNGs. SP-800-22 [33] is developed by NIST and it is the most-applied battery for RNG evaluation.

The output of a test on a bit string is another random variable with a given distribution of probability, the so-called *test statistic*. Hence, the $\mathcal{P}$ value; namely, the probability of getting an equal or worse test statistic, satisfying the i.i.d. hypothesis, are computed. If the $\mathcal{P}$ values are smaller than some *a priori* defined critical values, then the tests are considered failed: these limits are usually chosen as $\mathcal{P} < 0.01$ and $\mathcal{P} < 0.001$, corresponding to a confidence level of 99% and 99.9%, respectively. Otherwise, whenever one obtains $\mathcal{P}$ values equal or greater than these limits, the i.i.d. hypothesis for the tested string is assessed.

In Table I we report the results applied on the secure bits extracted by measuring a qubit and a ququart, respectively. All the tests are passed.

[1] T. Jennewein, U. Achleitner, G. Weihs, H. Weinfurter, and A. Zeilinger, Rev. Sci. Instrum. **71**, 1675 (2000).
[2] M. Fiorentino, C. Santori, S. M. Spillane, R. G. Beausoleil, and W. J. Munro, Phys. Rev. A **75**, 032334 (2007).
[3] W. Wei and H. Guo, Opt. Lett. **34**, 1876 (2009).
[4] K. Svozil, Phys. Rev. A **79**, 054306 (2009).
[5] M. Fürst, H. Weier, S. Nauerth, D. G. Marangon, C. Kurtsiefer, and H. Weinfurter, Opt. Express **18**, 13029 (2010).
[6] M. Jofre, M. Curty, F. Steinlechner, G. Anzolin, J. P. Torres, M. W. Mitchell, and V. Pruneri, Opt. Express **19**, 20665 (2011).
[7] R. Gallego, L. Masanes, G. De La Torre, C. Dhara, L. Aolita, and A. Acín, Nat. Commun. **4**, 2654 (2013).
[8] C. Abellán, W. Amaya, M. Jofre, M. Curty, A. Acín, J. Capmany, V. Pruneri, and M. W. Mitchell, Opt. Express **22**, 1645 (2014).
[9] S. Pironio, A. Acín, S. Massar, A. B. de la Giroday, D. N. Matsukevich, P. Maunz, S. Olmschenk, D. Hayes, L. Luo, T. A. Manning, and C. Monroe, Nature (London) **464**, 1021 (2010).
[10] C. Dhara, G. Prettico, and A. Acín, Phys. Rev. A **88**, 052116 (2013).
[11] R. Colbeck, Ph.D. thesis, University of Cambridge, 2006.
[12] R. Colbeck and A. Kent, J. Phys. A: Math. Theor. **44**, 095305 (2011).
[13] U. Vazirani and T. Vidick, Philos. Trans. R. Soc., A **370**, 3432 (2012).
[14] S. Pironio and S. Massar, Phys. Rev. A **87**, 012336 (2013).
[15] R. Colbeck and R. Renner, Nat. Phys. **8**, 450 (2012).
[16] D. Frauchiger, R. Renner, and M. Troyer, arXiv:1311.4547.
[17] A. De, C. Portmann, T. Vidick, and R. Renner, SIAM J. Comput. **41**, 915 (2012).
[18] R. Konig, R. Renner, and C. Schaffner, IEEE Trans. Inf. Theory **55**, 4337 (2009).
[19] Y. Zhao, C.-H. F. Fung, B. Qi, C. Chen, and H.-K. Lo, Phys. Rev. A **78**, 042333 (2008).
[20] L. Lydersen, C. Wiechers, C. Wittmann, D. Elser, J. Skaar, and V. Makarov, Nat. Photonics **4**, 686 (2010).
[21] F. Xu, B. Qi, and H.-K. Lo, New J. Phys. **12**, 113026 (2010).
[22] L. Lydersen, V. Makarov, and J. Skaar, Phys. Rev. A **83**, 032306 (2011).
[23] M. Tomamichel and R. Renner, Phys. Rev. Lett. **106**, 110506 (2011).

[24] J. M. Renes and J. C. Boileau, Phys. Rev. Lett. **103**, 020402 (2009).
[25] M. Berta, M. Christandl, R. Colbeck, J. M. Renes, and R. Renner, Nat. Phys. **6**, 659 (2010).
[26] H. Maassen and J. B. M. Uffink, Phys. Rev. Lett. **60**, 1103 (1988).
[27] D. Holste, I. Große, and H. Herzel, J. Phys. A: Math. Gen. **31**, 2551 (1998).
[28] N. J. Beaudry, T. Moroder, and N. Lütkenhaus, Phys. Rev. Lett. **101**, 093601 (2008).
[29] O. Gittsovich, N. J. Beaudry, V. Narasimhachar, R. R. Alvarez, T. Moroder, and N. Lütkenhaus, Phys. Rev. A **89**, 012325 (2014).
[30] F. Steinlechner, P. Trojek, M. Jofre, H. Weier, D. Perez, T. Jennewein, R. Ursin, J. Rarity, M. W. Mitchell, J. P. Torres, H. Weinfurter, and V. Pruneri, Opt. Express **20**, 9640 (2012).
[31] F. Steinlechner, S. Ramelow, M. Jofre, M. Gilaberte, T. Jennewein, J. P. Torres, M. W. Mitchell, and V. Pruneri, Opt. Express **21**, 11943 (2013).
[32] L. Trevisan, J. Assoc. Comput. Mach. **48**, 860 (2001).
[33] A. Rukhin *et al.*, NIST Special Publication 800-22 Revision 1a (2010).
[34] P. L'Ecuyer and R. Simard, AACM Trans. Math. Software **33**, 22 (2007).